International Journal of Recent Technology and Engineering (IJRTE)
ISSN: 2277-3878 (Online), Volume-8, Issue-1, May 2019

Fuzzy and Objectiveness Integrated Optimization of Extended Topological Active Net for Multi Object Segmentation

Pramila B, M B Meenavathi

Abstract: ***Image segmentation partitions an image to multiple objects. Topological Active Nets (TAN) and its extension Extended Topological Active Nets (ETAN) deforms meshes and composes them to fit to the objects to be segmented applying energy functional optimization. ETAN leads to local optima in cases of complex images with holes in it or with complex curves. In this work, an integrated fuzzy rule based learning and objectiveness measurement is used to optimize the ETAN. Fuzzy rule base is derived from training images for which segmented result is available as ground truths. Fuzzy rule base aids in decision for placement of links at segmentation boundaries. Objectiveness is foreground connectivity measure learnt with Laplacian Gaussian filter and used in decision for deletion of links in mesh for fitting complex shapes.***

Keywords: ETAN, Fuzzy rule base, Objectiveness and TAN.

I. INTRODUCTION

Deformable models (DM) [1] are the curves and surfaces over image and the surfaces deform due to internal and external forces. The smoothness during deformation is maintained by internal forces and orientation towards the objects of interest in image is maintained by external forces. Topological Active Net (TAN) [2] is a geometric deformable model implementing a elastic two dimensional mesh. The mesh has matrix with interrelated nodes. Energy functional based mesh deformation is done in TAN till the energy function reaches minimum value. The minimum value is reached when the model is over the objects. The problem of image segmentation is solved as mathematical function with goal of energy minimization. It is defined as

$$v(m,n) = \big(x(m,n), y(m,n)\big)$$

where $(m,n)\varepsilon[[0,1]X[0,1]$

The mesh deformation is controlled by energy function below

$$E\big(v(m,n)\big) = \int_0^1 \int_0^1 [E_{int}\big(v(m,n)\big) + E_{ext}\big(v(m,n)\big)]dmdn$$

Revised Manuscript Received on 30 May 2019.
***** Correspondence Author
Pramila B*, Department of EIE, Bangalore Institute of Technology College (BIT) Bengaluru, Karnataka India.
Dr M.B. Meenavathi, Prof. & Head, Department of EIE, Bangalore Institute of Technology College (BIT) Bengaluru, Karnataka India.

Where the internal energy $Eint$ control contraction and bending and defined as

$$E_{int}(v(m,n)) = \alpha(|v_m(m,n)|^2+|v_n(m,n)|^2) + \beta(|v_{mm}(m,n)|^2 + |v_{mn}(m,n)|^2) + |v_{nn}(m,n)|^2)$$

The partial derivatives are denoted as subscripts in above equation and the first and second order smoothness of net is optimized using coefficients α, β. First order derivatives are computed using following equations

$$|v_m(m,n)|^2 = [\,||d_m^+(m,n)||^2 + ||d_m^-(m,n)||^2]/2$$
$$|v_n(m,n)|^2 = [\,||d_n^+(m,n)||^2 + ||d_n^-(m,n)||^2]/2$$

The forward (d^+) and backward (d^-) differences are computed as follows

$$d_r^+(m,n) = [v(m+k,s) - v(m,n)]/k$$
$$d_r^-(m,n) = [v(m,n) - v(m-k,n)]/k$$
$$d_s^+(m,n) = [v(m,n+l) - v(m,n)]/l$$
$$d_s^-(m,n) = [v(m,n) - v(m,n-l)]/l$$

The second order derivatives are computed as

$$v_{mm}(m,n) = \frac{v(m-k,n) - 2v(m,n) + v(m+k,n)}{k^2}$$
$$v_{nn}(m,n) = \frac{v(m,n-l) - 2v(m,n) + v(m,n+l)}{l^2}$$
$$v_{mn}(m,n) = \frac{v(m-k,n) - v(m-k,n+l) - v(m,n) + v(m,n+l)}{kl}$$

The external energy represents the features of the scene and is given as

$$E_{ext}\big(v(m,n)\big) = \omega f\big[I\big(v(m,n)\big)\big] + \frac{\rho}{|N(m,n)|}\sum_{p\varepsilon N(m,n)} \frac{1}{||v(m,n) - v(p)||} f[I\big(v(p)\big)]$$

Where ω,ρ are the weights, $I\big(v(m,n)\big)$ is the value of intensity of pixel at position $v(m,n)$. $N(m,n)$ is the neighborhood of node at (m,n). Function f is defined as

$$f\big[I\big(v(m,n)\big)\big] = \begin{cases} Imax - \dfrac{\gamma^{\overrightarrow{I(v(m,n))}}}{\overrightarrow{I(v(m,n))+}} + \varepsilon(Gmax - \\ -G(v(m,n))) + \Phi GD(v(m,n)) \end{cases}$$

Where $_{\gamma}, \varepsilon, \Phi$ are the weighting terms, $Imax, Gmax$ are the maximum intensity values of image I and the gradient image G. $I(v(m,n)), G(v(m,n))$ are the intensity values of original image and gradient image at position $v(m,n)$. $\overrightarrow{I(v(m,n))}$ is the mean intensity in n*n square mask.

TAN works by placing the mesh over the whole image and apply energy minimization on each node in mesh to deform it and fit to the objects. Greedy search is done to find the optimal solution. Energy of node and its neighborhood in its current position is computed at each step. Node moves to position of lowest energy value. The algorithm stops when there nodes cannot be moved further. TAN mesh fails for the cases of complex concavities and convex shapes. It is because of restriction in the TAN regarding the links. Links cannot be deleted and links has to follow shape constraints in TAN. TAN problems are solved using ETAN. ETAN propose a new external energy term to guide the mesh and function f is updated from TAN as

$$f[I(v(m,n))] = \begin{cases} {}^{\gamma}\overrightarrow{I(v(m,n))} \\ Imax - \overrightarrow{I(v(m,n))} \end{cases} + \varepsilon(Gmax - -G(v(m,n)))+\Phi DG_{evfc}(p)$$

Where

$$DG_{evfc}(p) = \frac{1}{\sum_{q \varepsilon NW(p)} |q|}$$

For certain shapes, the mesh links need to be cut. ETAN cuts the links based on energy threshold. The links energy is calculated as

$$E_{link} = (\sum_{p \varepsilon A} DG_{evfc}(p).\frac{I(p)}{I_{max}}) / |A|$$

A is area for which energy is computed and p is the pixel in that area. The original image is given as I and the maximum intensity value is given as I_{max} The cutting threshold is fixed as the mean energy of the links. Holes are identified starting from misplaced internal nodes. For every internal node r(n) is calculated as

$$r(n) = \frac{E_{ext}(n)}{E_{ext}(n) + E_{int}(n)}$$

Where E_{ext} is the external energy and E_{int} is the internal energy of the node n. The node with highest ratio is selected and if its r value is higher then threshold for holes, a hole in opened starting from this node. The energy for all links starting from this node and to the neighbors are calculated and highest one is removed. Like this way more links can be deleted from the mesh and adjusted to the edge of the object.

ETAN and TAN has be extended using many optimization methods in the view of reducing time complexity and increase the segmentation accuracy. Our work is one such with application of fuzzy rule based learning and objectiveness measurement to optimize the ETAN. For accurate evolution of the ETAN mesh, the links lying on the background pixels and at boundary of the object must be removed. The link removal process in ETAN is complex as it has to iteratively remove each link at the neighborhood of node with highest r(n) value. To solve this problem in removal of links for creating holes, this work proposed a fuzzy rule base and objectiveness integrated solution to remove many links and nodes at a time. Due to the hole creation process and link removal process around the edge of object is speeded up without losing accuracy of the segmentation.

RELATED WORK

The existing optimizations for TAN and ETAN are discussed in this section.

In [3] author applied genetic operator for TAN optimization. Mutation operation were defined to generate mesh models with no cross links among the nodes. With GA, the local minima lock up problem is minimized and it works specifically well with noisy images.

In [4] proposed a hybrid optimization applying GA with Best Improvement Local Search (BILS). This method performed better than GA proposed in [3], but it requires a huge computation time as the consequence of huge population size needed for proper operation of GA. Author applied a evolutionary approach with goal of multi objective optimization [5] to avoid complex parameter tuning but still the computation time was not reduced.

In [6] author applied an ETAN optimization solution based on scatter search. A new energy term is introduced in this work. Due to it, segmentation accuracy of ETAN is increased. Even though the accuracy of segmentation improved time complexity was not reduced in a greater way in this approach.

In [7] authors applied micro-differential evolution (DE) to replace the deterministic search in the best improvement local search method to improvise the directional guidance. Using historical information, the micro population is tuned to find potentially promising search directions. This step improves the probing process to find the promising neighbor region for each node in TAN.

In [8] deformation optimization of TAN though Artificial Neural Networks (ANN) obtained using evolutionary algorithm is proposed. ANN is trained for movement of internal and external nodes in TAN. Trained ANN is applied to each node in steps and stopped when final segmentation is obtained. The approach is characterized by high computational complexity.

In [9] proposed an automatic division procedure for TAN mesh using a hybrid algorithm. The hybrid algorithm combined genetic and greedy algorithm. The solution allowed division of active net to multiple subnets with each corresponding to an object in the image. The approach could not adjust mesh structure for the case of concavities in the image.

In [10] proposed genetic optimization of ETAN. Two optimization algorithms namely Dual surface minimization (DSM) and hybrid of real coded genetic algorithms greedy algorithm (GAGR) are proposed in this work. The initialization sensitivity is increased due to global energy optimization. The proposed algorithms are able to extract surface from noise volumetric image. But the mesh is not able to segment multiple objects in the image.

In [11] authors applied Genetic algorithm to solve the problems in deformable models. It addresses initialization, pose estimation and local minima problems. It does it through parallel evolution of a multiple models. To reduce the search space in the evolution, constraints is placed in form of statistics based deformation. The time complexity is high in this approach.

In [12] author proposed a unification model. This model is proposed to solve the local minima problem in active contour method. The unification models involve snake model, the Rudin-Osher-Fatemi denoising model and the Mumford-Shah's segmentation model. Through dual formulation, the problem of active contour propagation towards object boundaries is solved. Energy functions were expressed in terms of level set. The approach is able to reduce the computation time by avoiding re-initializing the active contours periodically, but the approach fails for complex shapes.

In [13] authors proposed a block evolution method to improve the contour evolution. Nuclear norm minimization constraints are imposed on the evolution of active contour models. Due to this shape conformability of contour is maintained and large deformation of adjacent curves is avoided. The solution is able to increase the robustness of active contour models.

In [14] authors proposed a multiphase active contour model for segmenting brain MRI images. The methods work well for segmenting images with multiple regions of different mean intensity value like that of gray and white matter in brain MRI images. Applying globally convex formulation of Vese and Chan and a efficient dual minimization scheme, multiple contour are derived with each fitting a object to be segmented. The approach works well only for certain category of images.

In [15] authors proposed a new active contour model. It used higher-order diffusion for segmentation of image with intensity in-homogeneities for further optimization. The model was able to converse to edge due to use of gradient and Laplace information. It works well for the case of images with weak object boundaries.

II. FUZZY AND OBJECTIVENESS INTEGRATED OPTIMIZATION

The proposed ETAN optimization applies two concepts of Objectiveness and Fuzzy learning based rule base. The segmentation process in illustrated in the figure below

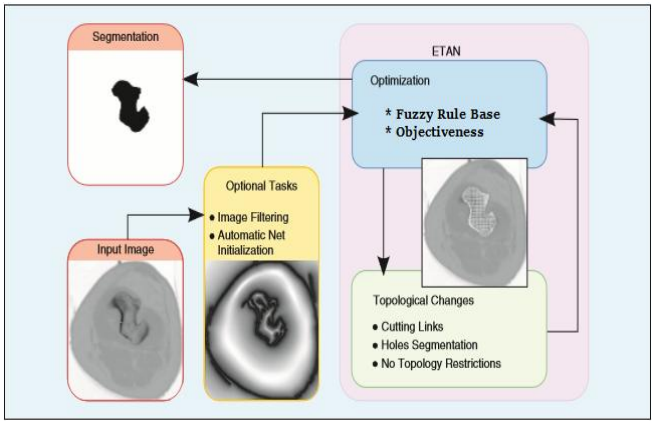

Figure 1 Segmentation Process

(a) Objectiveness based Optimization

Objects in image are recognized using well defined closed boundaries and centers. Objectiveness is a measure of how likely an active mesh subnet is in foreground. The subnet lying on background should be removed. Different from previous approaches of deleting mesh links one by one, a subnet is removed as whole in this work speeding up the topology change due to holes creation and alignment to object surface.

Over the entire image mesh is placed and mesh is split to window of size nXn. For each window, a filter is applied to calculate the objectives score. Laplacian of a Gaussian filter of size 5X5 is applied. Areas of rapid changes in image(like edges) are detected with Laplacian filter. To reduce the noise sensitivity, image smoothing is done by applying Gaussian filter before Laplacian. This two step process is referred as Laplacian of Gaussian (LoG).

$$L(x,y) = \nabla^2 f(x,y) = \frac{\partial^2 f(x,y)}{\partial x^2} + \frac{\partial^2 f(x,y)}{\partial y^2}$$

To include smoothing, Gaussian and Laplacian is combined in one equation as

$$LoG(x,y) = -\frac{1}{\Pi\sigma^2}(1 - \frac{x^2+y^2}{2\sigma^2})e^{\frac{x^2+y^2}{2\sigma^2}}$$

For uniform image, LoG value will be 0. When change occurs, LoG gives as positive or negative response depending on darker side or lighter side.

For approximating the effect of LoG following approximate discrete convolution kernel is used.

$$\begin{bmatrix} 0 & 0 & 1 & 0 & 0 \\ 0 & 1 & 2 & 1 & 0 \\ 1 & 2 & -16 & 2 & 1 \\ 0 & 1 & 2 & 1 & 0 \\ 0 & 0 & 1 & 0 & 0 \end{bmatrix}$$

The 2-D LoG for different values of σ is shown below

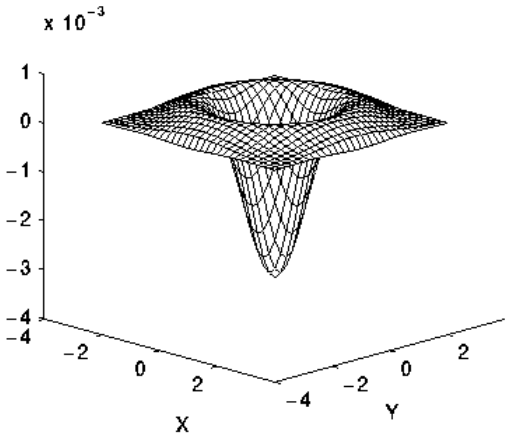

Figure 2 LoG Function

The objectiveness score for pixel is calculated from the Gaussian window as

$$PixObj(p) = \sum_{i=1}^{k} SiLoG(x,y)$$

Where Si is the objectiveness score of the windows containing pixel p and $LoG(x,y)$is the LOG value of the Gaussian window with x,y as the relative coordinate of the pixel p.

The Ob (Objectiveness) score for a the whole of window region is calculated by summing the pixel wise objectiveness score, It is given as

$$\mathrm{Ob(R)} = \sum_{i \epsilon R} PixObj(p)$$

The Ob(R) value is thresholded (T) to decide if the region R is the part of foreground. If Ob(R) is below the threshold, then the mesh in that region is removed as background. The value of Threshold (T) is obtained by calculating Ob(R) for known set images split to patches and from the results, the best Ob(R) value which characterizes even a small object presence is decided as the threshold for isolation of background from foreground region.

(b) Fuzzy Rule Base based Optimization

Once an active mesh is on the surface of intensity image, the links of the mesh can be categorized as below

1. Links Completely within the object
2. Links at boundary of object and background.
3. Links at the background

The links at the boundary must be removed, so that the remaining links represents the object. To speed the process of removing of the links, the links must be first classified. A Fuzzy rule based classifier is trained using a training set of images whose links results are known and expressed as ground truths.. The fuzzy rules are derived in the form of features of link against the class label for the link. Each class label represents one of three link positions defined above. Gaussian function is generated as output class label. Representing as Gaussian function is advantageous as the parameters of the function can be updated simultaneously during the training and the membership of link is modeled as fuzzy decision with probability of presence in each class instead of making a hard decision of associating a link to a particular class.

For the links in the training images, the links are labeled as 0, 1, and 2 corresponding to link within object, at the boundary or at the background. For each link, four features are extracted.

1. Local minima of a link (f1)
2. Thickness of a probable edge (f2)
3. LoG value around the starting node (f3)
4. LoG value around the ending node (f4)

Local minima for a link AB is calculated as follows.

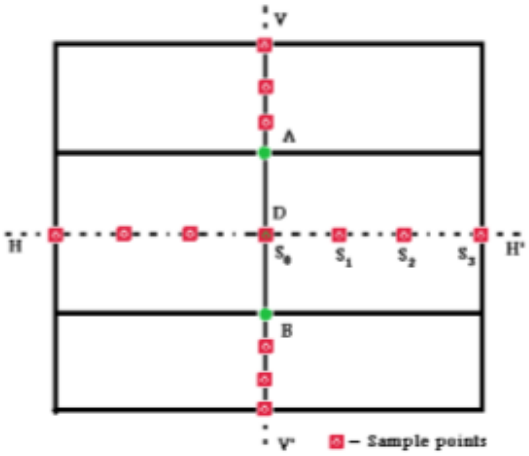

Figure 3 Link Diagram

With D as the middle of AB, the horizontal direction HH' is split to equal spaced points along the span of the next neighbor link. If the intensity distribution along S0,S1,S2… are monotonically increasing , the difference between the initial and final sampling point is taken as candidate feature for the direction of DH'. In case S0, S1, S2… are not monotonically increasing, the candidate feature value for the direction of DH' is taken as 0. Similarly the feature values along DH, DV, DH' is taken and the maximum of these values is taken as local minima of the link.

Thickness of a probable edge is calculated as follows:

For each of axis(DH', DH, DV, DV') the maximum range of monotonically increasing or decreasing value of the sampled points is taken and the minimum of these four values is the indication of thickness of probable edge at the boundary.

LoG is calculated with Laplacian of a Gaussian filter of size $5X5$ around the starting node A and the ending node B. It indicates the presence of edges near the nodes A and B.

The training dataset consist of features set of N links (f1, f2, f3, f4) against the label for it [0, 1, 2]. Fuzzy C Means clustering on done on the dataset with C=3. The cluster center after the fuzzy C means clustering is defined as

$$C = \{ C_{e,q}\ , e = 1,2,3\ and\ q = 1,2,3,4,5\}$$

Where $C_{e,q}$ is the qth coordinate of the eth cluster.

The closeness of the qth feature of the rt^{h} link f $_{r,q}$ with qth coordinate of eth cluster is defined using Gaussian function as

$$G\left(f_{r,q}, C_{e,q}, \sigma_{e,q}\right) = e^{\frac{(f_{r,q}-C_{e,q})^2}{\sigma_{e,p}{}^2}}$$

Where

$$\sigma_{e,q} = \frac{1}{N_e}\sum_{r=1}^{N_e}(f_{r,q} - C_{e,q})^2$$

The closeness of features of r[th] link to the e[th] cluster is given as

$$\Psi_{r,e} = \prod_{q=1}^{P} G(f_{r,q}, C_{e,q}, \sigma_{e,q})$$

The output label for e[th] cluster is found from the linear regression of input features $f_{r,q}$ as

$$\Phi_{r,e} = W_{e,0} + \sum_{q=1}^{P} W_{e,q,f_{r,q}}$$

Where W is the regression coefficient of the e[th] cluster. Since each of the r[th] link has membership value to all three clusters, final label of that particular link is given by weighting the label of the link with its membership value as

$$\bar{N}(r) = \sum_{e=1}^{3} \Psi_{r,e}\Phi_{r,e}$$

The value of $\bar{N}(r)$ calculated above may have a error with respect to $N(r)$ from training. The total error is calculated as

$$E = \sum_{r=1}^{N} ||\bar{N}(r) - N(r)||^2$$

The Gaussian parameters $C_{e,q}, \sigma_{e,q}$ and the regression coefficients $W_{e,p}$ are tuned to reduce the error defined above using gradient decent method.

$$C_{e,q}(t+1) = C_{e,q}(t) + \eta_C \frac{\partial E}{\partial C_{e,q}}$$

$$\sigma_{e,q}(t+1) = \sigma_{e,q}(t) + \eta_\sigma \frac{\partial E}{\partial \sigma_{e,q}}$$

$$W_{e,q}(t+1) = W_{e,q}(t) + \eta_W \frac{\partial E}{\partial W_{e,q}}$$

Where t is the iteration number and $\eta_C, \eta_\sigma, \eta_W$ are the learning parameters. The iteration is stopped when error threshold is reached.

From training the Fuzzy Gaussian membership functions are obtained for each class. During the segmentation, for each link in the active mesh, the four features are calculated and from it the fuzzy membership function for each class is found. For the membership over 70% as background the link is removed. For the membership of over 70% as boundary the node is moved to boundary and the link is shortened.

(c) Optimized ETAN

The overall procedure of the optimized ETAN is given below

Given an image to segment, the mesh is laid over whole image. The entire are is split to N*X*N window and for each window objectives score is calculated. For regions with objectiveness score less than objectiveness threshold, the mesh is removed in that region. In the rest of region, each link, the features (f1, f2, f3, and f4) is calculated and the link is classified to determine the membership class. Based on membership class of the link, the link is removed as defined in actions based on fuzzy rule base. After both of the process, ETAN energy minimization is done on each sub mesh,

$$(v(m,n)) = \int_0^1 \int_0^1 [E_{int}(v(m,n)) + E_{ext}(v(m,n))]dmdn$$

The overall process of optimization is given below

Figure 4 Optimization Process

IV.RESULTS

The proposed solution was tested against images of

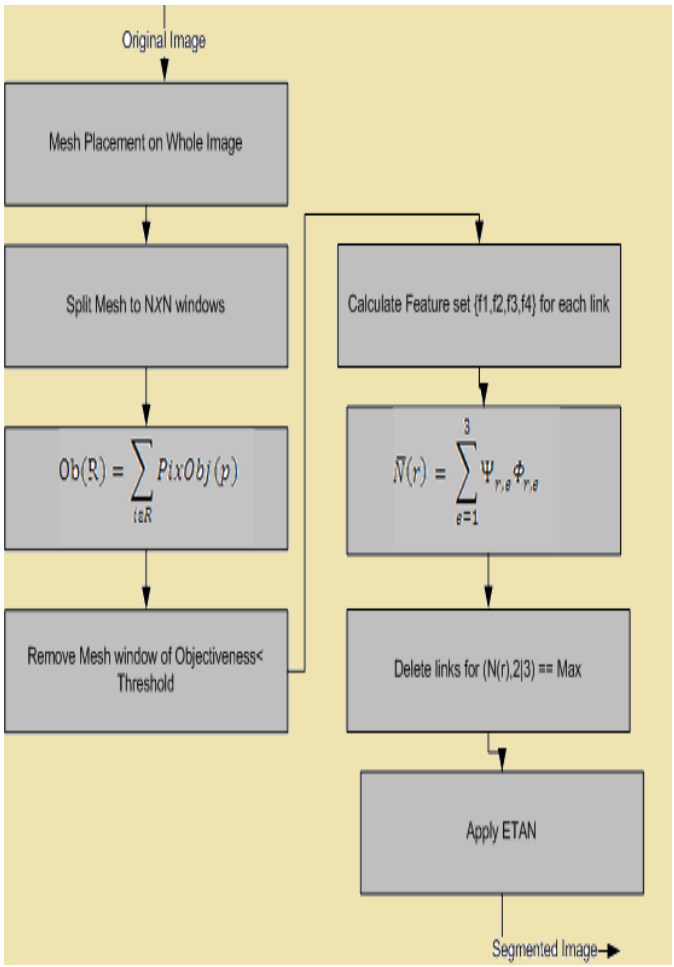

different categories and for comparison; the original ETAN (without any optimization) and ETAN-EBLIS are used. For each image to be tested a ground truth image in terms of expected segmentation result is created and structural similarity between the segmented result and the ground truth image is done.

The performance is measured in terms of two parameters

1. Spatial Accuracy Index (SAI)
2. Structural Similarity Index (SSIM)
3. Segmentation time
4. Hausdorff distance

Spatial Accuracy Index is calculated as

$$SAI = \frac{C(R \cap T)}{C(R) + C(T)}$$

Where R is the segmentation result, T is the ground truth and $C(X)$ is the cardinality of X which is measured in terms of number of pixels it contains.

Structural Similarity Index is calculated as

$$SSIM(x,y) = \frac{(2\mu_x\mu_y + C_1)(2\sigma_{xy} + C_2)}{(\mu_x^2 + \mu_y^2 + C_1)(\sigma_x^2 + \sigma_y^2 + C_1)}$$

Where

μ_x	Mean of x
σ_x	Variance of x
σ_{xy}	Co variance of x,y
X	Segmented result(Actual result)
Y	Ground truth (Expected result)

Segmentation time is the time taken for segmentation.

Hausdorff distance is the maximum distance between two contours

$$d_H(R,T) = max\begin{cases}\sup\inf d(r,t), r\varepsilon R^{t\varepsilon T} \\ \sup\inf d(r,t), t\varepsilon T^{r\varepsilon R}\end{cases}$$

It measures the worst case of segmentation. Lower value of $d_H(R,T)$ indicates higher effectiveness of segmentation.

The results of segmentation for different category of images are given below

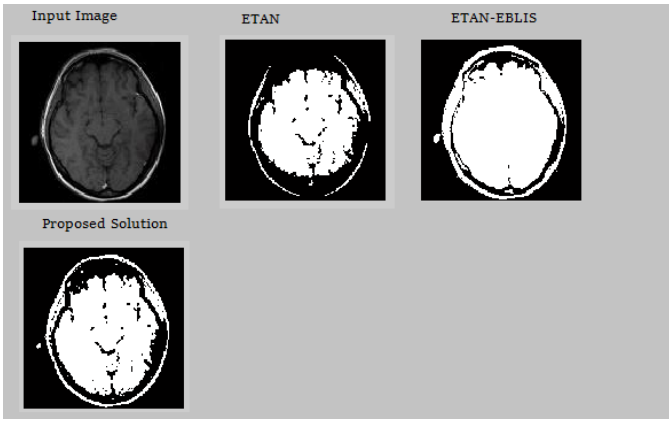

Figure 5 Result Comparison 1

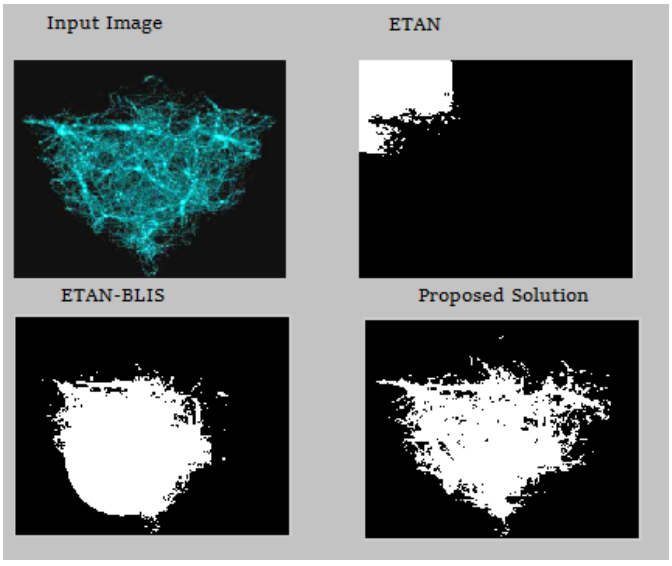

Figure 6 Result Comparison 2

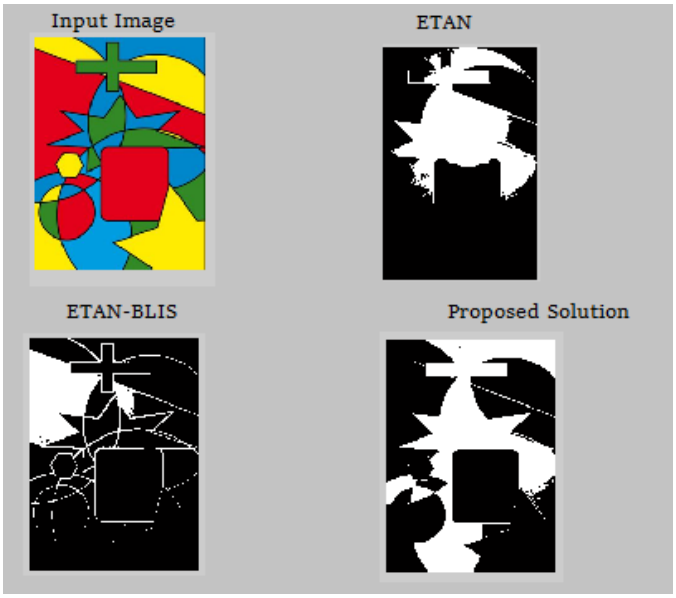

Figure 7 Result Comparison 3

The three solutions of Proposed, ETAN and ETAN-BLIS were tested against 20 images each from the following dataset.

1. MSRA-1000 dataset [16]
2. CSSD dataset [17]

MSRA dataset is selected for its simple and image with versatile content and background. CSSD dataset has images with high structural complexity. Segmented results obtained using the proposed solution is evaluated against the ground-truth images created using human effort.

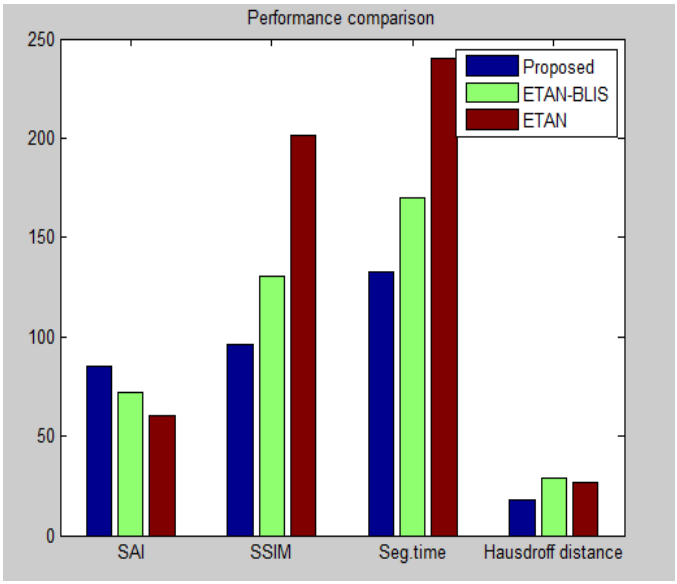

Figure 8 Performance Comparison

Table 1 Performance Results

Solution	SAI	SSIM	Avg Segmentation time	Hausdorff distance

Proposed Solution	0.85	96.28	133 ms	18
ETAN	0.6	201.15	240 ms	37
ETAN-BLIS	0.72	130.17	170 ms	29

From the results, it can seen that SAI value is higher in the proposed solution when compared to ETAN and ETAN-BLIS, demonstrating the closeness of segmentation result with ground truth in case of proposed. SSIM value is lower in the proposed solution as the segmentation boundaries are close to ground truth. The segmentation time is reduced in proposed due to reduction in mesh space for which energy must be minimized due to fuzzy and objectiveness optimization. The Hausdorff distance is lowest in the proposed demonstrating the effectiveness of segmentation.

V. CONCLUSION

In this work, an integrated approach consisting of objectiveness and fuzzy rule base is proposed to optimize the ETAN. Due to reduction of mesh to sub mesh based on objectives and fuzzy rule based link removal, the subsequent ETAN process is optimized in terms of running time and accuracy of segmentation. The comparison results with original ETAN and ETAN-EBLIS were encouraging. The reduction in running time and the increase in accuracy with the ground truth values is demonstrated for various categories of images. The proposed work works on intensity levels of pixels and as future work, texture information can be used to change the topology of mesh. Texture analysis will make the object recognition even more robust and can be used to further adapt the topology in removal of further links and restructure the nodes position to further reduce the time for segmentation and at a same for increased segmentation accuracy.

REFERENCES

1. D. Terzopoulos “Deformable models”. The Visual Computer, 4:306–331, 1988
2. M. Bro-Nielsen, “Active nets and cubes,” IMM, Tech. Rep., 1994.
3. O. Ibanez, J.Santos, and M. G. Penedo, “Genetic approaches for topological active nets optimization,” Pattern Recognition., vol. 42, no. 5, pp. 907–917, 2009.
4. J. Novo, J. Santos, “Topological active models optimization with differential evolution,” Expert Syst. Appl., vol. 39, no. 15, pp. 12165–12176, 2012.
5. J. Novo, M. Penedo, “Evolutionary multiobjective optimization of topological active nets,” Pattern Recogniton., Lett., vol. 31, no. 13, pp. 1781–1794, 2010.
6. N. Bova, O. Cordón, “Image segmentation using extended topological active nets optimized by scatter search,” IEEE Comput. Intell. Mag., vol. 8, no. 1, pp. 16–32, Feb. 2013.
7. Li, Yuan-Long ,Qing. “.Fast Micro-Differential Evolution for Topological Active Net Optimization” IEEE transactions on cybernetics. 46. 10.1109/TCYB.2015.2437282.
8. Cristina V. Sierra, Jos´e Santos "Emergent Segmentation of Topological Active Nets by Means of Evolutionary Obtained Artificial Neural Networks" In Proceedings of the 5th International Conference on Agents and Artificial Intelligence (ICAART-2013).
9. N. Barreira,M. J. Santos "Automatic Topological Active Net Division in a Genetic-Greedy Hybrid Approach": Pattern Recognition and Image Analysis 2007.
10. Tohka, J.: “Global optimization of deformable surface meshes based on genetic algorithms.” In: Proceedings ICIAP, pp. 459–464. IEEE Computer Society Press, Los Alamitos (2001).
11. C. McIntosh, G. Hamarneh, "Medial-based deformable models in nonconvex shape-spaces for medical image segmentation", *IEEE Trans. Med. Imag*, vol. 31, no. 1, pp. 33-50, 2012.
12. X. Bresson, J.-P. Thiran, and S. Osher, “Fast global minimization of the active contour/snake model,” J. Math. Imag. Vis., vol. 28, no. 2, pp. 151–167, Jun. 2007.
13. Guoqi Liu , Haifeng Li, “Robust Evolution Method of Active Contour Models and Application in Segmentation of Image Sequence,” Journal of Electrical and Computer Engineering, vol. 2018, 11 pages, 2018.
14. Juan C. Moreno,V. B. S. Prasath "Brain MRI Segmentation with Fast and Globally Convex
15. Multiphase Active Contours" arXiv,28 Aug 2013.
16. Guodong Wang , Jie Xu, "Active Contour Model Coupling with Higher Order Diffusion for Medical Image Segmentation",Int J Biomed Imaging. 2014.
17. Radhakrishna Achanta, Francisco Estrada, and Sabine S¨usstrunk, “Frequency-tuned salient region detection,” 2009, pp. 1597–1604.
18. Qiong Yan, Li Xu, “Hierarchical saliency detection,” in IEEE Conference on Computer Vision and Pattern Recognition, 2013, pp. 1155–1162

AUTHORS PROFILE

Pramila B is research Scholar from Visvesvaraya Technological University, Belgaum pursing at, Department of EIE, BIT, Bangalore-04.

Dr M.B. Meenavathi, Prof. & Head, Department of EIE, BIT, Bangalore-04, has 29 years of Teaching experience and has 14 publications. She is a member of IMSTE and IAENG. Her area of interest is Image processing, signal processing and fuzzy logic.